Production of bio-derived ethyl lactate on GaUSY zeolites prepared by post-synthetic galliation

Author(s):
Dapsens, Pierre Y.; Menart, Martin J.; Mondelli, Cecilia; Pérez-Ramírez, Javier

Publication date:
2014-02

Permanent link:
https://doi.org/10.3929/ethz-a-010792703

Originally published in:
Green Chemistry 16(2), https://doi.org/10.1039/c3gc40766g

Funding acknowledgement:
140496 - Biomass to chemicals over tailored hierarchical zeolite-based catalysts (SNF)

Green Chemistry

Dynamic Article Links ►

Cite this: DOI: 10.1039/c0xx00000x

www.rsc.org/xxxxxx

COMMUNICATION

Production of bio-derived ethyl lactate on GaUSY zeolites prepared by post-synthetic galliation

Pierre Y. Dapsens, Martin J. Menart, Cecilia Mondelli* and Javier Pérez-Ramírez*

Received (in XXX, XXX) Xth XXXXXXXXX 20XX, Accepted Xth XXXXXXXXX 20XX

DOI: 10.1039/b000000x

Galliation of USY zeolites in alkaline media creates tetra-coordinated Lewis-acid centres linked to the framework which display outstanding selectivity in the isomerisation of dihydroxyacetone to ethyl lactate and full reusability. This simple and affordable post-synthetic route enables to tune the amount of Lewis acidity in the zeolite and has great potential for application in related biomass conversions.

In recent years, the production of green solvents derived from renewable resources, *i.e.* biomass, has gathered substantial interest.[1,2] In this context, the synthesis of bio-based ethyl lactate (EL) attracts particular attention since this medium could replace to a significant extent conventional solvents, especially toxic halogenated hydrocarbons.[3] Nowadays, EL is industrially attained by H_2SO_4-catalysed esterification of lactic acid (LA) with ethanol.[4] Two main drawbacks are associated with this process: (i) thermodynamic limitations, which make it that high-purity EL streams can be obtained only by applying multifunctional reactors and continuous water extraction, and (ii) the utilisation of a homogeneous and highly corrosive acid catalyst, which implies environmentally unattractive and costly neutralisation and separation steps.[3] Recently, the Lewis-acid heterogeneously catalysed isomerisation of dihydroxyacetone (DHA) in ethanol has been identified as a sustainable alternative for EL production.[5-7] The reaction network comprises the dehydration of DHA into pyruvaldehyde (PAL), followed by an intramolecular rearrangement of the latter into the desired EL product (Scheme 1).[7,9] While the additional presence of weak Brønsted-acid centres in the catalyst favours the reaction by promoting the first step, the coexistence of strong Brønsted acidity appears detrimental as it drives the transformation of the PAL intermediate into the undesired pyruvic aldehyde diethyl acetal (PADA).[9] Tin-containing porous solids (*e.g.* Sn-beta, Sn-MCM-41, and Sn-CSM) have shown a remarkable performance in this isomerisation, enabling the full conversion of DHA into EL at

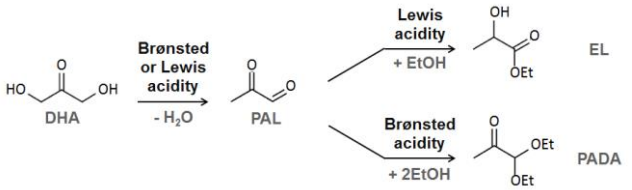

Scheme 1 Reaction scheme of the acid-catalysed conversion of dihydroxyacetone to ethyl lactate.

363 K within 4-6 h.[9-11] Nevertheless, the scarce worldwide availability of tin and the lack of proven large-scale synthesis protocols hampers at present their industrial implementation.[1] The performance of commercially available aluminosilicate zeolites in DHA isomerisation has also been investigated.[7,12] Pescarmona et al.[7] have established a linear relationship between the EL yield and the amount of extraframework aluminium (EFAl) in Y, ultra-stable Y (USY), ZSM-5, and beta zeolites. At 363 K, a maximum EL yield of 59% was reached over CBV600 (H-USY bulk Si/Al = 2.6), thus being significantly inferior to that obtained with tin-based materials.

With the aim of generating highly selective tin-free catalysts, our group has recently explored the potential of post-synthetic modification of commercial zeolites as an affordable and industrially amendable strategy to tailor their native acidic and porous properties. We could demonstrate that desilication of MFI-type zeolites in aqueous NaOH leads to hierarchical systems able to isomerise DHA in water into lactic acid with a selectivity comparable to the state-of-the-art catalyst, Sn-beta.[13] This is due to the creation of unique Lewis-acid sites by redistribution of a fraction of the pristine lattice aluminium in ZSM-5 upon alkaline treatment.[13,14] These selective centres also formed in silicalite-1 by alkaline treatment in the presence of a soluble aluminium source such as $Al(NO_3)_3$.[13] Unfortunately, the reusability of the catalysts was limited since the Lewis-acid Al sites introduced were progressively washed out from the solid due to the low pH of the lactic acid-rich mixture. Herein, we have transposed this approach to FAU-type zeolites to boost their performance in the conversion of DHA into ethyl lactate. Thanks to the lower polarity of ethanol and the non-acidic nature of the product, the inconvenience of catalyst instability should vanish.[9] We show that desilication in the presence of a soluble aluminium or gallium salt, *i.e.* alkaline-assisted metallation, serves well to the purpose. In particular, we emphasise the facile synthesis of GaUSY catalysts, which display the highest EL selectivity reported so far for any tin-free material, 82% at 358 K, and are fully reusable.

CBV720 (H-USY bulk Si/Al = 17, denoted as P) was selected as parent zeolite instead of CBV600, as this material undergoes appreciable modification upon alkaline treatment under milder conditions due to the lower aluminium content in the zeolite.[15] CBV720 features a micropore volume (V_{micro}) of 0.29 $cm^3\ g^{-1}$ and an external surface area (S_{meso}) of 128 $m^2\ g^{-1}$ (Table 1). TEM imaging evidences the presence of some mesoporosity (see

Table 1 Characterisation data of the zeolites

Catalyst[a]	Si/Al[b] (mol mol^{-1})	Si/Ga[b] (mol mol^{-1})	Cryst.[c] (%)	V_{micro}[d] (cm^3 g^{-1})	S_{meso}[d] (m^2 g^{-1})
P	17	–	100	0.29	128
AT	8	–	0	0.03	312
ATAl1	10	–	27	0.10	303
ATAl2	9	–	7	0.14	216
ATAl3	8	–	27	0.17	182
ATAl4	8	–	51	0.26	161
ATAl5	7	–	78	0.23	138
ATGa1	9	19	23	0.05	361
ATGa2	10	10	57	0.20	245
ATGa3	12	9	57	0.21	220
ATGa4	15	7	88	0.24	137
ATGa5	14	7	80	0.25	119

[a] P = parent CBV720, AT = alkaline treatment with 0.2 M NaOH, Al*x*/Ga*x* = AT in the presence of 0.0*x* M of $Al(NO_3)_3$/$Ga(NO_3)_3$. [b] Determined by ICP-OES. [c] Crystallinity derived from XRD. [d] Determined by the *t*-plot method.

arrows in Fig. 1, P), which originates from the dealumination by steam and acid leaching of the pristine Y. Alkaline treatment in 0.2 M NaOH (code AT) was effective in increasing the S_{meso} by a factor of 2.5, but simultaneously induced the collapse of the zeolite lattice, as indicated by the significant drop of V_{micro} (Table 1) and the total loss of crystallinity evidenced by TEM and XRD (Fig. 1, AT and Fig. SI1). As mentioned above, alkaline treatment of silicalite-1 in the presence of aluminium cations enabled to quantitatively introduce selective Lewis-acid centres while partially preserving its crystallinity.[13,16] Consequently, we explored the effect of such strategy on the FAU framework. Due to the fact that the metal source is external to the material, this post-synthetic approach has the advantage, compared to the simple base leaching of aluminosilicates, that the type and amount of Lewis sites can be tuned. In our case, gallium was considered besides aluminium. The use of gallium was already conceived a few decades ago in order to develop more efficient zeolites for the reforming, cracking, and aromatisation of hydrocarbons. Still, while its incorporation into a zeolitic framework was widely demonstrated by hydrothermal synthesis,[17-19] alkaline-assisted galliation has been hardly explored and led to different outcomes.[20-21] For instance, Liu et al. produced Ga-beta in aqueous NaOH,[20] but the same protocol applied to CBV780 caused the structural breakdown of the zeolite.[21] Through systematic addition of variable amounts of $Al(NO_3)_3$ or $Ga(NO_3)_3$ (0.01-0.05 M) to the alkaline solution, we have generated two classes of modified catalysts (ATAl*x* and ATGa*x* samples, respectively). Their compositional, structural, and porous properties are summarised in Table 1. The zeolite crystallinity was retained to a larger extent by increasing the concentration of the trivalent cations in the treatment. Although the effect of Ga^{3+} was in this respect more pronounced at lower molarities, a similar plateau value as high as *ca.* 80% was reached at 0.05 M for both metal cations. The variation of S_{meso} in ATAl*x* and ATGa*x* samples followed a reverse trend, *i.e.* it gradually decreased at higher salts concentrations. These results are expected since M^{3+} cations are known to act as pore directing agent (PDA), that is, to bind to the zeolite surface, regulating the process of Si extraction in the presence of hydroxyls ions and, thus, ultimately protecting the crystal from excessive dissolution.[16] The observed variations in crystallinity and mesoporosity are supported by TEM (Fig. 1, ATGa1 and ATGa4), as well as N_2 sorption and XRD data (Fig. SI1). The Si/Al and Si/Ga ratios progressively decreased from ATAl1/ATGa1 to ATAl5/ATGa5, confirming the substantial metal incorporation into the zeolite. Particularly, the use of $Ga(NO_3)_3$ instead of $Al(NO_3)_3$ as PDA enabled to quantitatively introduce more metal into the zeolite, as evidenced by the lower Si/M ratio of ATGa*x* compared to ATAl*x* samples (Table 1). Additionally, despite the significant amount of gallium contained

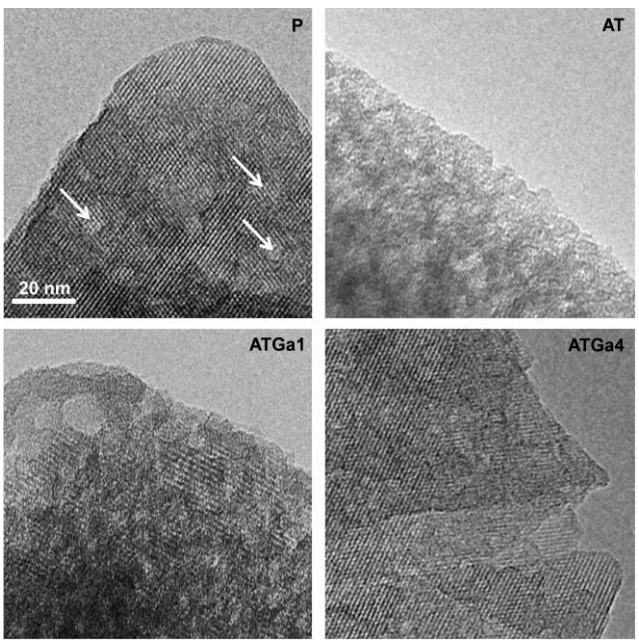

Fig. 1 Transmission electron micrographs of P and selected alkaline-treated zeolites. The scale bar applies to all micrographs.

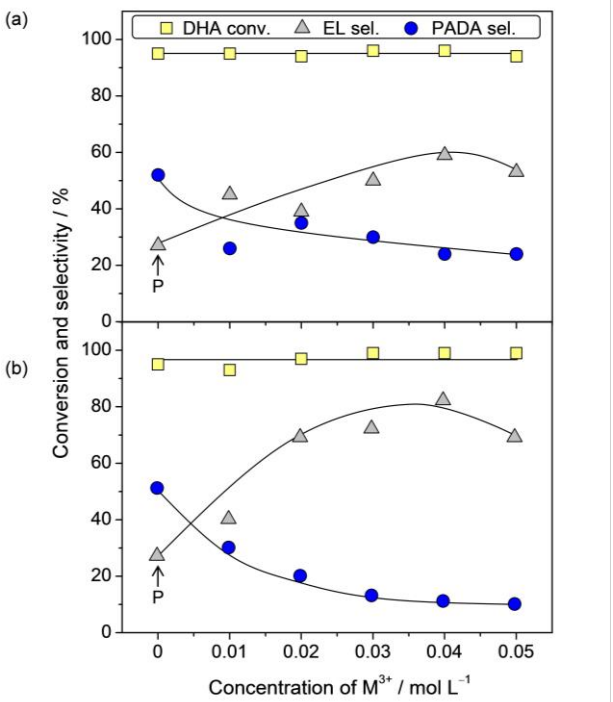

Fig. 2 Conversion of DHA and selectivity to EL and PADA versus the concentration of (a) $Al(NO_3)_3$ and (b) $Ga(NO_3)_3$ used during the alkaline treatment of P.

into ATGa4 (6 wt.% as determined by elemental analysis), no amorphous species were observed by TEM (Fig 1, ATGa4), suggesting that the metal should be mainly located into the zeolite structure (*vide infra*).

The parent and modified zeolites were evaluated in the isomerisation of DHA in ethanol at 358 K for 24 h (Fig. 2). In all of the cases, PADA was found as the main side-product besides EL (see Scheme 1). P afforded a rather low EL selectivity (27%) at 97% DHA conversion, consistent with previous data.[6] The alkaline-treated sample (AT) provided a similar EL selectivity but attained a DHA conversion level of only 85% (not shown). Remarkably, alkaline-assisted alumination and galliation of P led to an appreciable improvement of the performance (Fig. 2). In particular, almost full DHA conversion was observed over all of the samples and the EL selectivity progressively augmented, at the expense of that of PADA, along with the increase in concentration of the metal salt added upon base leaching up to 0.04 M. A higher M^{3+} concentration led to a slight decrease in selectivity. Interestingly, the EL selectivity was higher for the galliated samples. Accordingly, while the maximum EL selectivity was 59% for ATAl4, ATGa4 reached a value of 82%. This selectivity is the highest reported so far for any tin-free catalyst and greatly surpasses that of CBV600 evaluated under the same reaction conditions (*vide infra*).[7]

In order to understand the origin of the outstanding performance of samples galliated by post-synthetic alkaline treatment, acidity characterization by IR spectroscopy of adsorbed pyridine was applied. As depicted in Fig. SI2, the pyridine adsorption band at 1456 cm^{-1}, associated to Lewis acidity, gained progressively in intensity from P to ATGa5, corresponding to a total raise in Lewis-acid sites concentration from 52 to 139 μmol g^{-1}. On the contrary, the slight depletion of the band at 1545 cm^{-1} indicated a lowering of the amount of Brønsted-acid centres (from 215 to 195 μmol g^{-1}) (Fig. SI2). These evidences strongly point to gallium incorporation in the zeolite in form of Lewis-acid species. The shift of the Lewis acidity signal from 1456 to 1458 cm^{-1}, observed previously for isomorphously substituted Ga-zeolites,[22,23] additionally hints that they may be predominantly tetra-coordinated. As illustrated in Fig. 3, the selectivity to EL linearly correlated with the amount of Lewis-acid sites in the different catalysts. Noteworthy, the lower value obtained over ATAl4 is associated to its lower Lewis

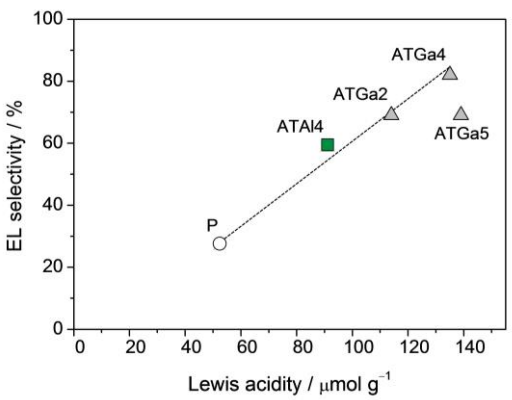

Fig. 3 Selectivity to EL versus the amount of Lewis-acid sites (probed by infrared spectroscopy of adsorbed pyridine) of CBV720 in parent form and after different post-synthetic treatments.

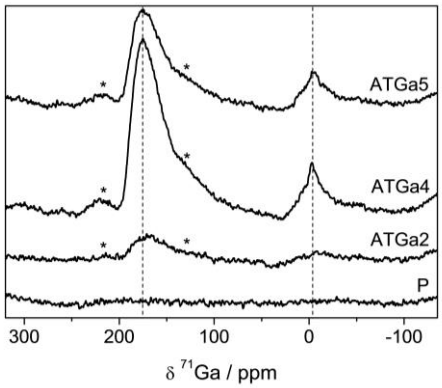

Fig. 4 ^{71}Ga MAS NMR spectra of parent and selected ATGax samples.

acidity (91 μmol g^{-1}), and is a consequence of the reduced amount of metal presented in ATAl*x* samples, as discussed earlier. Therefore, the nature of the metal salt used during alkaline-assisted metallation does not seem to play a key role in the EL selectivity. Interestingly, lower EL selectivity was attained over ATGa5 although this sample possessed similar Lewis acidity than ATGa4. Therefore, the Lewis acidity does not appear to be the only parameter driving the selectivity and the type of Lewis sites could be determinant. The nature of the Lewis centres was further investigated by ^{71}Ga MAS NMR. The spectra in Fig. 4 show two main peaks positioned at 175 and −2.5 ppm, associated to tetra-coordinated (Ga−Td) and hexa-coordinated (Ga−Oh) gallium species, respectively.[24,25] The higher intensity of the former signal indicates that gallium was mainly incorporated into Td positions, supporting the shift of the band in the infrared spectra. Interestingly, although ATGa4 and ATGa5 possessed the same bulk Si/Ga ratio (Table 1), 83% of Ga−Td was estimated for the former catalyst while only 79% for the latter. The less selective incorporation of trivalent cations into tetrahedral framework positions upon alkaline-assisted metallation at higher concentrations of M^{3+} species was already observed for silicalite-1.[16] Uncovering the precise origin of this interesting phenomenon requires a deeper understanding of the desilication mechanism than available at present. Nevertheless, considering that alkaline-assisted galliation relies on a fine balance between silica dissolution and gallium incorporation into the created vacancies, a too high concentration of Ga^{3+} likely leads to an easier healing of the vacancies, hindering further silicon removal and, thus, limiting the incorporation of gallium at tetrahedral sites. Based on the very low EL selectivity (48%) reached over commercial Ga_2O_3, *i.e.* Ga−Oh, Ga−Td species appear responsible for the selectivity of the process. To further substantiate this point, our best catalyst, *i.e.* ATGa4, was steamed, since the latter treatment is known to partially transform the coordination of trivalent species from tetrahedral into octahedral.[26] The EL selectivity of this sample decreased to only about half (from 82% to 48%). In analogy, the outstanding performance of Sn-containing zeolites in this reaction was demonstrated to originate from tetra-coordinated tin centres.[8] In light of these results, the difference in amount of Ga−Td species in the AT-Ga4 and AT-Ga5 zeolites, albeit small, may explain the slightly lower EL selectivity attained over the latter (Fig. 2). Current research efforts are directed towards a more precise elucidation of the nature of the highly selective tetra-coordinated Lewis-acid sites by means of

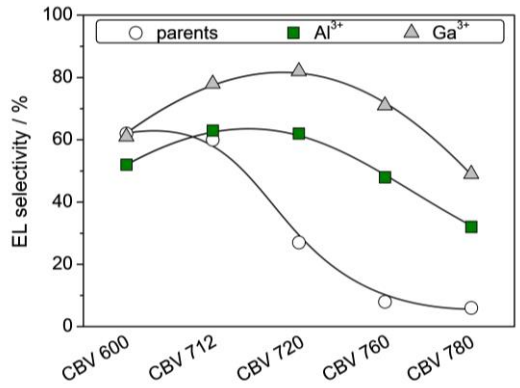

Fig. 5 Selectivity to EL over various commercial FAU-type zeolites (parents) and after alkaline treatment in the presence of 0.04 M $Al(NO_3)_3$ (Al^{3+}) or $Ga(NO_3)_3$ (Ga^{3+}).

high-field NMR techniques and DFT calculations.

In order to assess the application scope of alkaline-assisted metallation, the study was extended to other commercially available FAU-type zeolites with various Si/Al ratios, namely CBV600, 712, 760, and 780. The post-synthesis treatment of these samples was performed under the conditions found optimal for P, *i.e.* in the presence of 0.04 M of $Al(NO_3)_3$ and $Ga(NO_3)_3$ (Table SI1). Thereafter, the modified zeolites were evaluated under identical reaction conditions (Fig. 5). The EL selectivity over the parent zeolites diminished from CBV600 (EFAl-rich) to CBV780 (EFAl-poor), in line with the results by Pescarmona et al.[7] Although post-synthetic modification of CBV600 did not render a better performing catalyst, alumination and, even better, galliation of the other zeolites sensibly improved the selectivity. In particular, the higher the zeolite bulk Si/Al ratio, the greater was the increase in the EL selectivity upon alkaline-assisted metallation. This correlates well with recent work demonstrating the high stability of low Si/Al ratio (*e.g.* CBV600) in basic media and the high propensity of high Si/Al ratio FAU-type zeolites (*e.g.* CBV760) to be dissolved in aqueous NaOH.[15]

As recyclability is of paramount importance for potential industrial application, the performance of our best catalyst, ATGa4, was assessed in five consecutive runs. The catalyst was calcined prior to re-use in the following catalytic cycle. As evidenced in Fig. 6, the activity and selectivity levels remained constant. Furthermore, the original porous properties were fully preserved after the fifth run (not shown), highlighting the extreme

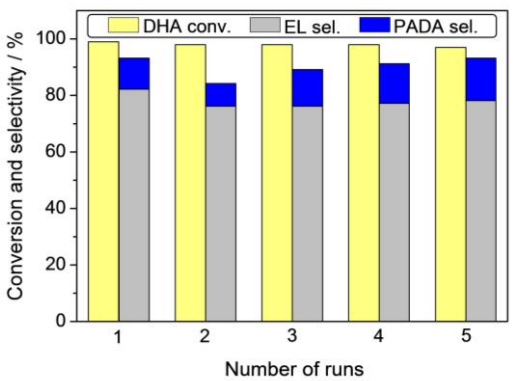

Fig. 6 Conversion of DHA and selectivity to EL and PADA upon reuse in four consecutive runs over ATGa4.

robustness of the galliated zeolite. This remarkable stability endows this novel class of catalysts with exciting perspectives of large-scale use. To this end, it is worth mentioning that the preparation of desilicated ZSM-5 zeolites was demonstrated at the pilot-scale (1.5 m^3),[27] thus highlighting the scalability of post-synthetic alkaline treatments. Moreover, no major aspect seems to hinder the production of galliated FAU zeolites at practical costs. Gallium-containing zeolites have indeed already reached industrial implementation, as exemplified by the Cyclar process.[28]

Conclusion

Highly selective and reusable catalysts for the isomerisation of dihydroxyacetone to ethyl lactate have been generated by alkaline treatment of commercial FAU-type zeolites in the presence of a soluble gallium salt. The EL selectivity of 82% at almost full DHA conversion presented in this work is the highest reported so far for any tin-free catalyst and is demonstrated to originate from the insertion of gallium in form of tetra-coordinated species, which feature enhanced Lewis acidity. These results reinforce the potential of post-synthetic modification of commercial zeolites as a powerful tool for the design of industrially viable catalysts for the production of bio-based chemicals. Preliminary results indicate that alkaline-assisted galliation can be successfully applied to other frameworks and that the thus modified USY zeolites attain exceptional selectivities also in the isomerisation of DHA into other valuable short-chain alkyl lactates. Thus, the alkaline-assisted metallation methodology herein developed is expected to be widely used in view of generating highly active tin-free catalysts in the isomerization of other bio-derived substrates such as hexoses and pentoses.

Acknowledgments

This work was supported by the Swiss National Science Foundation (Project Number 200021-140496). Dr. R. Verel and M. Valla are acknowledged for the fruitful discussions on ^{71}Ga MAS NMR data. Dr. S. Mitchell is thanked for TEM analysis.

Notes and references

Institute for Chemical and Bioengineering, Department of Chemistry and Applied Biosciences, ETH Zurich, Wolfgang-Pauli-Strasse 10, CH-8093 Zurich, Switzerland.
E-mails: jpr@chem.ethz.ch, cecilia.mondelli@chem.ethz.ch;
Fax: +41 44 6331405; Tel: +41 44 6337120

† Electronic Supplementary Information (ESI) available: Details on catalyst preparation, characterisation, and testing. XRD patterns and N_2 isotherms of selected samples, and IR of adsorbed pyridine of representative galliated catalysts. See DOI: 10.1039/b000000x/

1 P. G. Jessop, *Green Chem.*, 2011, **13**, 1391.
2 P. Y. Dapsens, C. Mondelli, J. Pérez-Ramírez, *ACS Catal.*, 2012, **2**, 1487.
3 C. S. M. Pereira, V. M. T. M. Silva, A. E. Rodrigues, *Green Chem.*, 2011, **13**, 2658.
4 C. S. M. Pereira, S. P. Pinho, V. M. T. M. Silva, A. E. Rodrigues, *Ind. Eng. Chem. Res.*, 2008, **47**, 1453.
5 Y. Román-Leshkov, M. E. Davis, *ACS Catal.*, 2011, **1**, 1566.
6 M. S. Holm, S. Saravanamurugan, E. Taarning, *Science*, 2010, **328**, 602.

7 P. P. Pescarmona, K. P. F. Janssen, C. Delaet, C. Stroobants, K. Houthoofd, A. Philippaerts, C. De Jonghe, J. S. Paul, P. A. Jacobs, B. F. Sels, *Green Chem.*, 2010, **12**, 1083.

8 E. Taarning, S. Saravanamurugan, M. S. Holm, J. M. Xiong, R. M. West, C. H. Christensen, *ChemSusChem*, 2009, **2**, 625.

9 F. de Clippel, M. Dusselier, R. Van Rompaey, P. Vanelderen, J. Dijkmans, E. Makshina, L. Giebeler, S. Oswald, G. V. Baron, J. F. M. Denayer, P. P. Pescarmona, P. A. Jacobs, B. F. Sels, *J. Am. Chem. Soc.*, 2012, **134**, 10089.

10 L. Li, C. Stroobants, K. Lin, P. A. Jacobs, B. F. Sels, P. P. Pescarmona, *Green Chem.*, 2011, **13**, 1175.

11 C. Hammond, S. Conrad, I. Hermans, *Angew. Chem., Int. Ed.*, 2012, **51**, 11736.

12 R. M. West, M. S. Holm, S. Saravanamurugan, J. Xiong, Z. Beversdorf, E. Taarning, C. H. Christensen, *J. Catal.*, 2010, **269**, 122.

13 P. Y. Dapsens, C. Mondelli, J. Pérez-Ramírez, *ChemSusChem*, 2013, **6**, 831.

14 V. Calsavara, E. Falabella Sousa-Aguiar, N. R. C. Fernandes Machado, *Zeolites*, 1996, **17**, 340.

15 D. Verboekend, G. Vilé, J. Pérez-Ramírez, *Adv. Funct. Mater.*, 2012, **22**, 916.

16 D. Verboekend, J. Pérez-Ramírez, *Chem. Eur. J.*, 2011, **17**, 1137.

17 R. M. Barrer, J. W. Baynham, F. W. Buttitude, W. M. Meier, *J. Chem. Soc.*, 1959, 195.

18 J. Selbin, R. B. Mason, *J. Inorg. Nucl. Chem.*, 1961, **20**, 222

19 D. J. Rawlence, K. Karim, J. Dwyer, *US Patent US5238675*, 1993.

20 X. Liu, J. Lin, X. Liu, J. M. Thomas, *Zeolites*, 1992, **12**, 936.

21 Th. L. M. Maesen, J. A. R. van Veen, D. A. Cooper, I. M. van Vegchel, J. W. Gosselink, *J. Phys. Chem. B*, 2000, **104**, 716.

22 N. A. S. Amin, D. D. Angogro, *J. Nat. Gas Chem.*, 2003, **12**, 123.

23 K. Karim, J. Dwyer, D. J. Rawlence, M. Tariq, A. Nabhan, *J. Mater. Chem.*, 1992, **2**, 1161.

24 H. K. C. Timken, E. Oldfield, *J. Am. Chem. Soc.*, 1987, **109**, 7669.

25 C. T. Chu, R. D. Partridge, S. E. Schramm, *US Patent US5057203*, 1991.

26 D. K. Simmons, R. Szostak, P. K. Agrawal, T. L. Thomas, *J. Catal.*, 1987, **106**, 287.

27 J. Pérez-Ramírez, S. Mitchell, D. Verboekend, M. Milina, N.-L. Michels, F. Krumeich, N. Marti, M. Erdmann, *ChemCatChem*, 2011, **3**, 1731.

28 S. S. Kjell, T.-H. Chao, N. J. Flint, A. A. Foutsitzis, *US Patent US4636483*, 1987.

Electronic Supplementary Information (ESI)

Production of bio-derived ethyl lactate on GaUSY zeolites prepared by post-synthetic galliation

Pierre Y. Dapsens, Martin J. Menart, Cecilia Mondelli* and Javier Pérez-Ramírez*

Institute for Chemical and Bioengineering, Department of Chemistry and Applied Biosciences, ETH Zurich, Wolfgang-Pauli-Strasse 10, CH-8093 Zurich, Switzerland. Fax: +41 44 6331405 Tel: +41 44 6337120; E−mails: cecilia.mondelli@chem.ethz.ch; jpr@chem.ethz.ch.

Catalyst preparation

The FAU-type zeolites employed throughout this study (CBV600, CBV712, CBV720, CBV760, and CBV780) were purchased from Zeolyst International and used as received for post-synthetic modification. The latter comprised alkaline treatment in aqueous 0.2 M NaOH (30 cm^3 per gram of dried zeolite) containing different concentrations (0-0.05 M) of $Al(NO_3)_3$ or $Ga(NO_3)_3$ (both purchased from Sigma, 99.9%) at 338 K for 30 min in an Easymax^{TM} 102 reactor (Mettler Toledo). The resulting materials were converted into the protonic form by three consecutive ion-exchanges in an aqueous solution of ammonium nitrate (0.1 M NH_4NO_3, 6 h, 298 K, 100 cm^3 per gram of dried zeolite) followed by calcination in static air at 823 K (5 K min^{-1}) for 5 h. A sample of the ATGa4 zeolite (particle size = 0.2-0.4 mm) was further steamed in a fixed-bed reactor (13 mm i.d.) under flowing water vapour in N_2 (30 cm^3 min^{-1} N_2, partial H_2O pressure 300 mbar) during 6 h at 823 K. All of the samples were used in the catalytic tests in their protonic form. Gallium (III) oxide (Strem Chemicals, 99.998%) was used as received.

Characterisation

The content of Si, Al, and Ga in the catalysts was determined by inductively coupled plasma optical emission spectroscopy (ICP-OES) in a Horiba Ultra 2 instrument equipped with a photomultiplier tube detector. Prior to the measurements, the materials were dissolved in aqueous 3.0 M NaOH under heating at 343 K for 3 h. Nitrogen sorption was performed at 77 K in a Quantachrome Quadrasorb-SI gas adsorption analyser on degassed samples (10^{-1} mbar, 573 K, 3 h). Powder X-ray diffraction (XRD) was conducted in a PANalytical X'Pert PRO-MPD diffractometer. Data were recorded in the 5-70° 2θ range with an angular step size of 0.05° and a counting time of 7 s per step. Infrared (IR) spectroscopy of adsorbed pyridine was performed in a Bruker IFS 66 spectrometer equipped with a liquid N_2-cooled MCT detector. Self-supporting zeolite wafers (5 tons cm^{-2}, 20 mg, 1 cm^2) were pretreated at 10^{-3}mbar and 693 K for 4 h. After cooling down to room temperature, the samples were saturated with pyridine vapour and then evacuated at room temperature for 15 min and subsequently at 473 K for 30 min. Spectra were recorded in the 4000-650 cm^{-1} range at 4 cm^{-1} resolution by co-addition of 32 scans. High-resolution magic angle spinning ^{71}Ga nuclear magnetic resonance (MAS NMR) spectroscopy was measured in a Bruker AVANCE 700 NMR spectrometer equipped with a 4-mm probe head and 4-mm ZrO_2 rotors at 213.5 MHz. Spectra were acquired using a spinning speed of 10 kHz, 20000 accumulations, 1 μs pulses, a recycle delay of 0.02 s, and a $Ga(NO_3)_3$ reference. Transmission electron microscopy (TEM) imaging was undertaken with a FEI Tecnai F30 microscope operated at 300 kV (field emission gun). The samples were prepared by depositing a few droplets of zeolites suspension in methanol on a carbon-coated copper grid, followed by evaporation at room temperature.

Catalytic tests

Catalytic tests were carried out batch-wise in 15-cm^3 thick-walled glass vials (Ace, pressure tubes, front seal) dipped in an oil bath at 363 K under autogenous pressure. The internal temperature recorded during the reactions was 358 K. The vials were loaded with 120 mg of dihydroxyacetone (DHA, Sigma-Aldrich, 97%, dimer), 80 mg of catalyst, and 3.88 g of ethanol (99.9%, Scharlau). The mixture was allowed to react under vigorous magnetic stirring for 24 h. After this time, the reaction was quenched in an ice bath and the catalyst removed by means of a Chromafil Xtra 0.25 μm syringe filter. The unconverted DHA was isolated by high-performance liquid chromatography (HPLC) in a Merck LaChrom system equipped with a Biorad Aminex HPX-87H column heated at 308 K, using an aqueous eluent of 0.005 M H_2SO_4 (pH 2) flowing at 0.6 $cm^3\ min^{-1}$. Quantification was obtained by integration of its UV-Vis absorbance band at 272 nm using methyl ethyl ketone as an internal standard. The produced ethyl lactate (EL) and pyruvic aldehyde diethyl acetal (PADA) were analysed using a gas chromatograph (GC, HP 6890) equipped with an HP-5 capillary column and a flame ionization detector. A He carrier gas flow rate of 4.3 $cm^3\ min^{-1}$ (pressure = 1.4 bar) and an injection size of 0.3 μL were used. The initial temperature of 328 K was held for 2 min before heating to 473 K (30 K min^{-1}). The yield of EL was determined using iso-octane as an internal standard, while that of PADA was determined utilising the response factor calculated for pyruvic aldehyde dimethyl acetal, since PADA was not commercially available. The conversion of DHA was calculated as the moles of DHA reacted divided by the moles of DHA fed, while the yields of EL and PADA were calculated as the moles EL and PADA formed, respectively, divided by the moles of DHA fed. Pyruvaldehyde and 1,1,2,2-tetraethoxypropane were identified as the other by-products by HPLC and GC-MS (GC, HP 6890, MS, HP 5973), respectively, but they were not quantified. No coke formation was detected. Reusability tests were performed at the above-described conditions. Between each run, the used catalyst was calcined in flowing air at 823 K (5 K min^{-1}) for 2 h. The testing of each catalyst was repeated three times. The experimental error for the reported conversion and selectivity values is ±1%.

Table SI1 Characterisation of the parent and treated zeolites.

Catalyst[a]	Si/Al[b] (mol mol^{-1})	Yield[c] (%)	Crystallinity[d] (%)	V_{pore} (cm^3 g^{-1})	V_{micro}[e] (cm^3 g^{-1})	S_{meso}[e] (m^2 g^{-1})	S_{BET}[f] (m^2 g^{-1})
CBV600	2.6	100	100	0.36	0.24	83	675
CBV600-ATAl4	–	81	87	0.45	0.24	128	717
CBV600-ATGa4	–	75	95	0.43	0.28	96	778
CBV712	6	100	100	0.48	0.28	113	807
CBV712-ATAl4	–	85	80	0.47	0.25	132	732
CBV712-ATGa4	–	90	82	0.48	0.28	99	783
CBV720	17	100	100	0.56	0.29	128	842
CBV720-ATAl4	–	89	51	0.54	0.26	161	795
CBV720-ATGa4	–	94	88	0.54	0.24	137	730
CBV760	30	100	100	0.56	0.31	149	903
CBV760-ATAl4	–	90	35	0.48	0.25	130	727
CBV760-ATGa4	–	78	67	0.64	0.25	194	812
CBV780	40	100	100	0.54	0.30	139	859
CBV780-ATAl4	–	72	0	0.34	0.08	162	335
CBV780-ATGa4	–	70	0	0.51	0.09	258	479

[a] The suffixes ATAl*x*/ATGa*x* indicate alkaline treatment with 0.2 M aqueous NaOH (338 K, 30 min) in the presence of 0.0*x* M of $Al(NO_3)_3$/$Ga(NO_3)_3$. [b] According to the manufacturer's specifications. [c] Based on the amount of solid recovered after alkaline treatment, ion-exchange, and calcination. [d] Crystallinity derived from XRD. [e] Determined by the *t*-plot method. [f] Determined by the BET method.

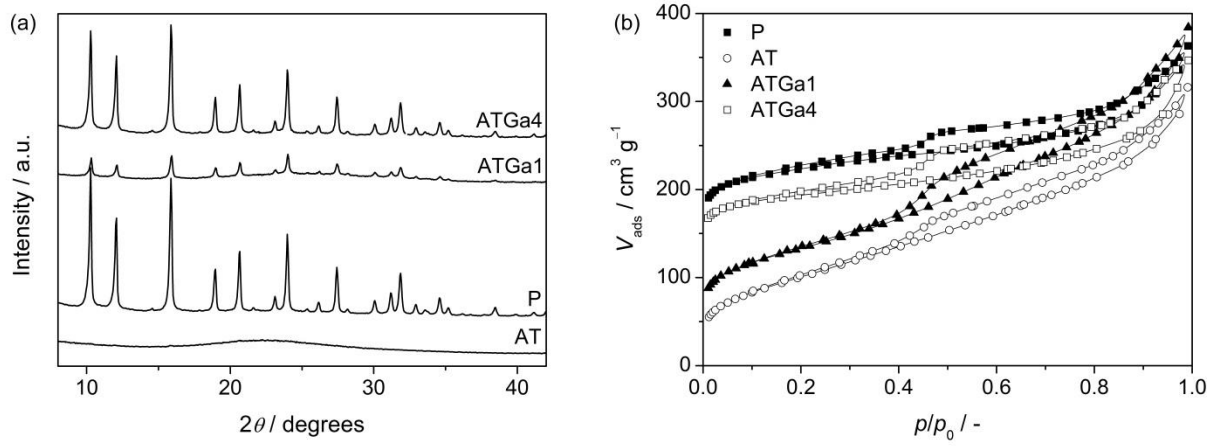

Fig. SI1 (a) X-ray diffraction patterns and (b) N_2 isotherms of CBV720 in parent form and after different post-synthetic treatments. The samples' codes are described in the caption of Table SI1.

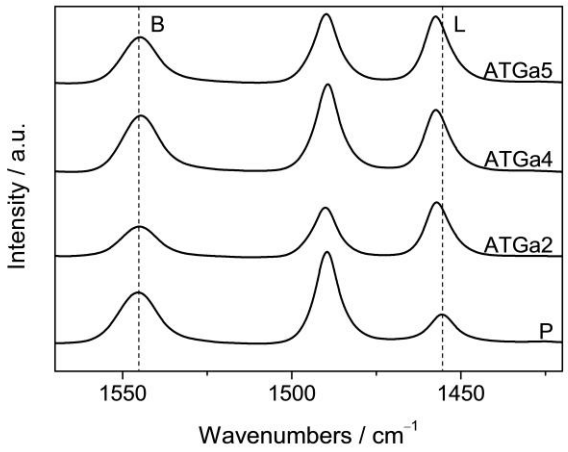

Fig. SI2 Normalized IR spectra of adsorbed pyridine of CBV720 in parent form and selected ATG*a*x samples. The samples' codes are described in the caption of Table SI1.